ISSN 1392–1320 MATERIALS SCIENCE (MEDŽIAGOTYRA). Vol. 17, No. 1. 2011

Negative Resistance Effect and Charge Transfer Mechanisms in the Ion Beam Deposited Diamond Like Carbon Superlattices

Andrius VASILIAUSKAS *, **Šarūnas MEŠKINIS**, **Sigitas TAMULEVIČIUS**

Institute of Materials Science of Kaunas University of Technology, Savanorių 271, LT-50131 Kaunas, Lithuania

Received 25 June 2010; accepted 02 February 2011

In the present study DLC:SiO_x/DLC/DLC:SiO_x/*n*Si and DLC:SiO_x/DLC/DLC:SiO_x/*p*Si structures were fabricated by ion beam deposition using a closed drift ion source. Current-voltage (I-V) characteristics of the multilayer samples were measured at room temperature. The main charge transfer mechanisms were considered. Unstable negative resistance effect was observed for some DLC:SiO_x/DLC/DLC:SiO_x/*n*Si and DLC:SiO_x/DLC/DLC:SiO_x/*p*Si structures. In the case of the diamond like carbon superlattices fabricated on *n*Si it was observed only during the first measurement. In the case of the some DLC:SiO_x/DLC/DLC:SiO_x/*p*Si negative resistance "withstood" several measurements. Changes of the charge carrier mechanisms were observed along with the dissapear of the negative resistance peaks. It seems, that in such a case influence of the bulk related charge transfer mechanisms such as Poole-Frenkel emission increased, while the influence of the contact limited charge transfer mechanisms such as Schottky emission decreased. Observed results were be explained by current flow through the local microconducting channels and subsequent destruction of the localized current pathways as a result of the heating by flowing electric current.

Keywords: diamond like carbon, superlattice, electrical properties, negative resistance, charge transfer mechanisms.

1. INTRODUCTION

Diamond like carbon (DLC) films received significant attention due to their outstanding mechanical, electrical and optical properties [1]. Particularly, present and prospective electronic applications of DLC films include electrically active passivation of high power electronics devices [2], material for fabrication of the membranes in microelectromechanical systems (MEMS) [3], piezoresistive [4 – 6] and electrochemical sensors [7]. Recently fabrication of the diamond like carbon based resonant tunnel diodes (RTD) operating at microwave frequencies range was reported in [8, 9]. Characteristic to the current-voltage relationship of a tunneling diode is the presence of one or more negative differential resistance regions, which enables many unique applications. Diamond like carbon based resonant tunnel diode (RTD) could find a lot of the potential applications in large area electronics due to the room temperature deposition possibility. However, in [8, 9] DLC based RTD structures were grown using complex method of the pulsed laser deposition and negative resistance effect in these structures was observed only at liquid nitrogen temperature.

In the present research multilayer DLC films were deposited by closed drift ion source which is already used in industry due to the large area deposition possibility and easy of maintenance. Current-voltage dependences of these structures were investigated and negative resistance effect observed for some samples at room temperature was analyzed in terms of charge transfer mechanisms.

2. EXPERIMENTAL

Multilayer diamond like carbon films (DLC superlattices) were deposited on n type and p type monocrystalline silicon (100) substrates by closed drift ion source. Silicon substrates before diamond like carbon growth were cleaned by degreasing in dimethylformamide and acetone. "Conventional" diamond like carbon (DLC) layers were deposited using acetylene gas. SiO_x containing diamond like carbon films (DLC:SiO_x) were deposited using mixture of the hexamethyldisiloxane vapor and hydrogen gas. Deposition rate of the DLC and DLC:SiO_x, established for thicker (~200 nm thickness) films, was 400 nm/h and 440 nm/h respectively. Dielectric permittivity of the DLC and DLC:SiO_x monolayer films of 200 nm thickness deposited on n-type silicon substrates was ~7 and ~3 respectively. Optical bandgap of DLC and DLC:SiO_x monolayer films of 200 nm thickness was ~1.2 eV and ~2.5 eV respectively. More details on the deposition conditions and structure of the multilayer DLC films (DLC superlattices) can be found in Table 1. It can be seen, that all DLC superlatices consisted of the narrow bandgap ultra-thin DLC layer inserted between the two ultra-thin wide bandgap DLC:SiO_x layers. This structure is typical for the resonant tunnel diode (RTD). Pulsed laser deposited diamond like carbon based RTD structure exhibiting negative resistance effect at liquid nitrogen temperature of the similar design was used in [8, 9].

After the DLC film synthesis, the samples were moved to the vacuum evaporation chamber as soon as possible. Top contacts were deposited onto the multilayer diamond like film via mask. The diameter of circular shaped top electrode was 500 μm. Afterwards bottom common electrodes were deposited onto the back surface of the silicon. Aluminum of 300 nm thickness was used as an electrode metal.

In present study Schottky emission [10, 11], Fowler–Nordheim tunneling, trap activated tunneling [12], space charge limited current [10, 11], Poole-Frenkel emission [10, 11] were considered as a possible charge transfer mechanisms. It should be mentioned, that in the case of the space charge limited current flow through the ideal defect-free dielectric $J \sim V^2$ current-voltage relationship will be

*Corresponding author. Tel.: +370-37-327605, fax.: +370-37-314423.
E-mail address: *sarunas.meskinis@ktu.lt* (A. Vasiliauskas)

Table 1. Deposition conditions and structure of the diamond like carbon superlattices.

Sample set name	Ion beam energy (eV)	Structure of diamond like carbon superlattice			Deposition time (s)			Thickness (nm)*		
		I layer	II layer	III layer	I layer	II layer	III layer	I layer	II layer	III layer
S414	800	$DLC:SiO_x$	DLC	$DLC:SiO_x$	40	10	40	5	1	5
S424	800	$DLC:SiO_x$	DLC	$DLC:SiO_x$	40	20	40	5	2	5
S434	800	$DLC:SiO_x$	DLC	$DLC:SiO_x$	40	30	40	5	3	5
S444	800	$DLC:SiO_x$	DLC	$DLC:SiO_x$	40	40	40	5	4	5
S222	800	$DLC:SiO_x$	DLC	$DLC:SiO_x$	25	20	25	3	2	3
S989	800	$DLC:SiO_x$	DLC	$DLC:SiO_x$	90	80	90	11	9	11
SL10	800	$DLC:SiO_x$	–	–	80	–	–	10	–	–
SL120	800	$DLC:SiO_x$	–	–	960	–	–	120	–	–

* approximate thickness calculated by using deposition rate of the thicker films.

observed [13], while $J \sim V^n$ with $n > 2$ dependence will be seen in the case of the space charge limited current with exponential traps distribution [14].

3. EXPERIMENTAL RESULTS

3.1. I-V characteristics and charge transfer mechanisms of the diamond like carbon superlattices on n-type silicon

For all the samples fabricated on n-Si, diode like current-voltage (I-V) characteristics were observed (Figs. 1, 2). Breakdown voltages were in 10 V – 35 V range (Fig. 1). For all the samples step-like breakdown (multiple breakdown events) can be seen. It can be explained by electrical breakdown via local defects (breakdown spots) similarly to the ultrathin silicon dioxide breakdown case [15]. It can be seen as well, that reverse I-V characteristics of the multilayer film samples are more scattered in comparison with the $DLC:SiO_x/n$Si heterostructures. It seems, that the breakdown voltage increases with thickness of both $DLC:SiO_x$ and DLC films in superlattice structure.

Leakage current of the almost all multilayer DLC/*n*Si heterostructures was lower than leakage current of the $DLC:SiO_x/n$Si heterojunction. However, for most S222 set samples and for some samples of other sets it was valid only at relatively low voltages due to the "soft" breakdown (Fig. 1, b).

In low current (10^{-7} A÷10^{-6} A) and voltages (0 V÷5 V) range, some kind of the current step can be seen for the most samples investigated. The most clearly it can be seen for $DLC:SiO_x/n$Si heterojunction. While in the case of some superlatice based samples of the S222 and S989 sets the step was absent.

Voltage of the turning point of the $DLC:SiO_x$/nSi was ~3 V when thickness of $DLC:SiO_x$ film was 10 nm and ~15 V when thickness of $DLC:SiO_x$ film was 120 nm. Current strength of the turning point of the $DLC:SiO_x$/nSi was ~0.45 μA when thickness of $DLC:SiO_x$ film was 10 nm and it was ~0.098 μA when thickness of $DLC:SiO_x$ film was 120 nm. It means, that some bulk-related charge transport mechanism at least partially should be responsible for such a phenomena [10, 11, 13, 14]. Turning point voltage for all the DLC superlattices and *n*Si heterojunction reverse characteristics was in (4.8 – 6.6) V range and turning point current strength was in (0.1 – 0.36) μA range. No clear relation between the position of the step turning point and structure of the DLC superlattices was observed.

The reverse I-V characteristics of the $DLC:SiO_x$/nSi heterostructures were stable versus time and cycles of measurements. While for the multilayer DLC and n-Si heterostructures in most cases some kind of degradation of the I-V characteristics was observed with number of measurements (Fig. 1, d).

Both contact-limited and bulk-limited charge transfer mechanisms such as Schottky emission, Fowler-Nordheim tunneling, trap activated tunneling as well as space charge limited currents (SCLC) and Poole-Frenkel emission were considered to reveal reasons of the peculiarities and stability of the I-V characteristics mentioned above.

Linear or quasilinear dependences were observed in the case of the Schottky, Poole-Frenkel and double logarithmic plots of the reverse I-V characteristics of the samples (Fig. 3). Additional analysis of these plots was performed. Effective dielectric permittivity was calculated from the slope of the linear parts of the Schottky and Poole-Frenkel plots. While in the case of the double logarithmic plot more precise analysis of the $J \sim V^n$ dependence has been made. It can be seen in Table 2, that in the low voltages range reasonable effective dielectric permittivity values was observed for Schottky plot, and effective dielectric permittivity values calculated from the Poole-Frenkel plot were higher (yet ε_{PF} of the single layer $DLC:SiO_x/n$Si heterostructure was close to the ε_{CV} of DLC and $DLC:SiO_x$ films). Slope of the double logarithmic plot at low voltages range was too high for space charge limited current case ($J \sim V^n$ with $n > 4.5$). At higher voltages (higher than voltage of the turning point of the I-V step) large or even negative values of the ε_{Sch} and ε_{PF} were observed. On the other hand $J \sim V^n$ dependence with n close to 1 can be seen in double logarithmic plot (quasilinear dependence). It means, that at low voltage (or low electric field strength range) Schottky emission is the main charge transport mechanism in multilayer DLC and *n*Si structures, while for the single layer $DLC:SiO_x/n$Si heterostructure Poole-Frenkel emission plays important role along with the Schottky emission. At higher reverse voltages charge transport can be described as a superposition of the space charge limited current ($J \sim V^2$ for ideal dielectric) and generation current ($J \sim V^{0.5}$).

Instability of the reverse I-V characteristics of the samples presented in Fig. 1, d, was considered in terms of the charge transport mechanisms as well. There were revealed, that in the case of the subsequent measurements (second, third, etc.) quasilinear regions of the double logarithmic plot can be described by $J \sim V^n$ function with

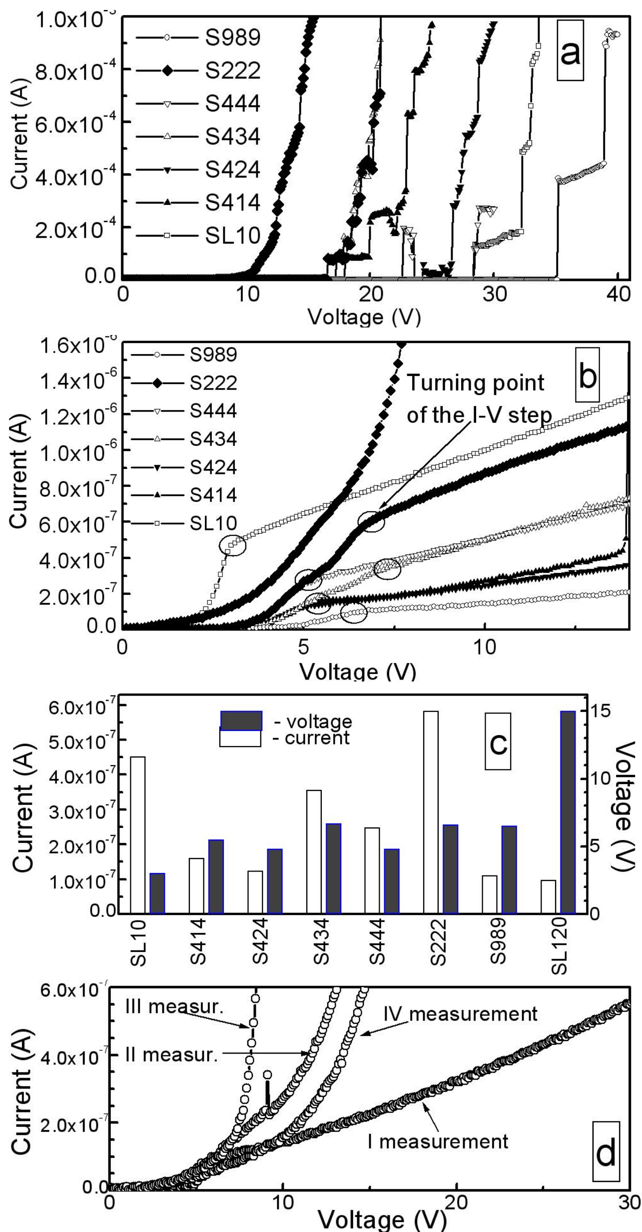

Fig. 1. Typical reverse current-voltage (I-V) characteristics of DLC:SiO_x/DLC/DLC:SiO_x/nSi samples: overall view (a), low current range (b); position of the turning point (c) and typical measurement induced changes of the reverse I-V characteristic (d)

$n > 3$. Analysis of the Schottky, Poole-Frenkel, Fowler-Nordheim and trap assisted tunneling plots was performed as well. There were revealed, that in the lower voltages range charge transport can be described as a superposition of the Schottky and Poole-Frenkel emission. On the other hand, exponentially distributed trap space charge limited current and, probably, Fowler-Nordheim emission can be considered at the higher voltage range. It seems, that electric current flow through the multilayer DLC film (DLC superlattice) results in formation of some additional defects. Such an effect was not observed for the single DLC:SiO_x/nSi heterostructure. Therefore, formation of the traps as a result of the damage of the "conventional" DLC interlayer in diamond like carbon superlattice can be supposed.

Typical forward I-V characteristics of the samples fabricated on n-type Si are presented in Fig. 2. In most cases some instability of the forward I-V characteristics was observed. In the case of the DLC:SiO_x/nSi heterostructure (film thickness 10 nm) I type forward I-V characteristics was observed – during the second measurement forward voltage decreased and no additional changes of I-V characteristic was observed during the next measurements. In the case of the multilayer DLC heterostructures with nSi for some samples some kind of the negative resistance effect was observed. It seems, that negative resistance phenomenon was more often observed in the case of the samples with thicker intermediate DLC interlayer (≥4 nm) – S444 and, especially, S989. However, negative resistance phenomenon was unstable – in all cases it was observed only during the first measurement.

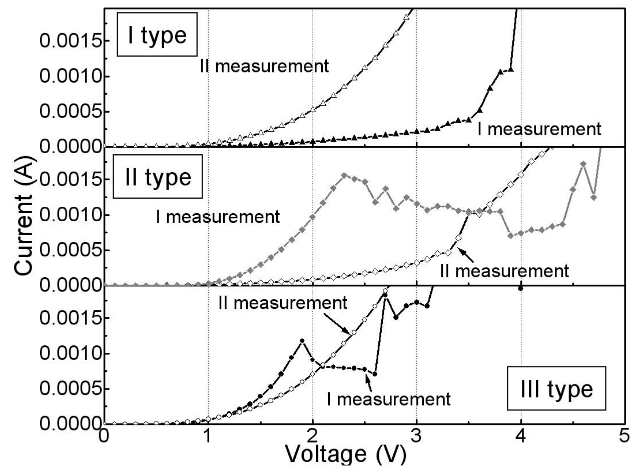

Fig. 2. Typical forward I-V characteristics of current-voltage (I-V) characteristics of DLC:SiO_x/DLC/DLC:SiO_x/nSi samples (presented I type I-V characteristic was measured for the sample from S444 set, II type – for the sample from S424 set and III type – for the sample from S414 set)

Study of the charge transport mechanisms was performed by using analysis of the I-V characteristics. Linear or quasilinear ranges were observed in Schottky, Poole-Frenkel, double logarithmic, Fowler-Nordheim tunneling and trap activated tunneling plots (Figs. 4, 5). The results of the analysis are presented in Table 3.

Analysis of I type (S444) I-V characteristics revealed, that in the low voltage range the main charge transfer mechanism is Schottky emission, at higher voltages – Schottky emission and space charge limited current with exponential trap distribution and at the highest voltages – possibly Fowler-Nordheim and/or trap activated tunneling. In the case of the second measurement at low voltages Schottky emission and Poole-Frenkel emission prevailed, at higher voltages – space charge limited current with exponential trap distribution as well as possibly Fowler-Nordheim and/or trap activated tunneling. Analysis of II type (S424) I-V characteristics revealed, that in the case of the first measurement in low voltages range (before negative resistance region) the main charge transfer mechanisms were Schottky emission and Poole-Frenkel emission as well as possibly Fowler-Nordheim and/or trap activated tunneling. In the case of the second measurementit was Poole-Frenkel emission, Schottky emission and space charge limited current with SCLC prevailing at higher voltages and Schottky emission as well as Poole Frenkel emission at lower voltages. Analysis of III type

Table 2. ε_{Sch}, ε_{PF} and n values of the reverse I-V characteristics of I-V characteristics of DLC:SiO_x/DLC/DLC:SiO_x/nSi samples

Sample's set	Electric field range (kV/cm)	ε_{Sch}	Electric field range (kV/cm)	ε_{PF}	Electric field range (kV/cm)	n in $J{\sim}V^n$
SL10	1400 – 3000	3.6	1400 – 3000	5.8	1400 – 3000	5.68
	3000 – 25000	937	3000 – 25000	<0	3000 – 25000	1.25
S434	3000 – 4000	5.6	3000 – 4000	46.7	3000 – 4000	5.60
	4000 – 5000	37.5	4000 – 5000	713	4000 – 6000	2.00
	5000 – 6500	178.4	5000 – 13000	86000	6000 – 13000	1.14
	6500 – 13000	440.6				
S444	2500 – 3600	5.4	2500 – 3600	33.2	2500 – 3600	5.95
	3600 – 15500	440	3600 – 15500	<0	3600 – 15500	0.97
S989	1500 – 2000	4.2	1500 – 2200	27.5	1500 – 2200	4.67
	2000 – 10000	215	2200 – 3000	<0	2200 – 3000	0.64
			3000 – 10000	21000	3000 – 10000	1.24

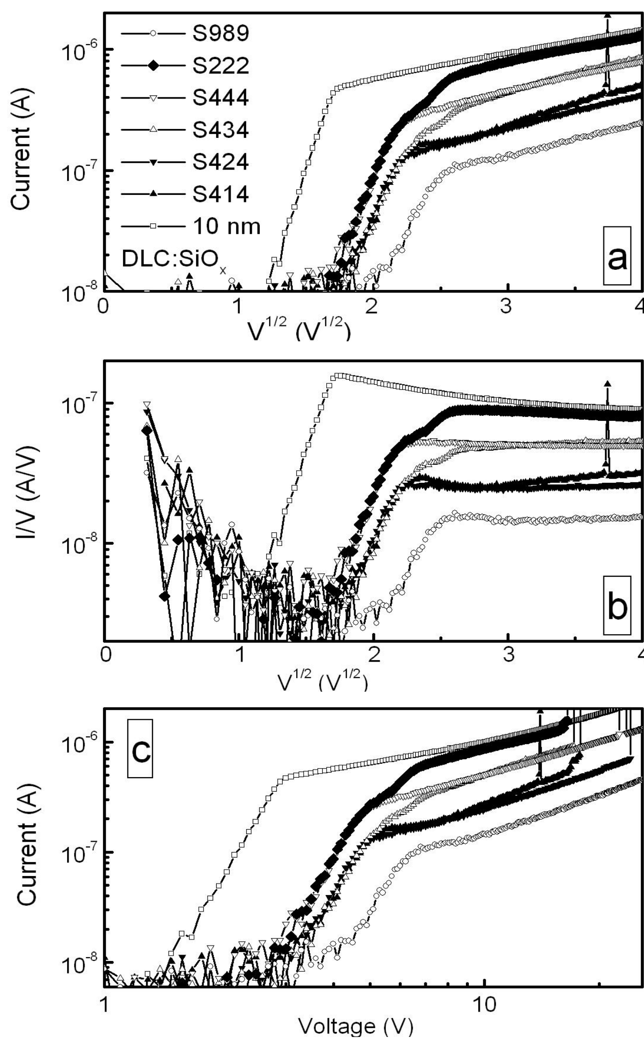

Fig. 3. Schottky (a), Poole-Frenkel and double logarithmic plots of current-voltage (I-V) characteristics of DLC:SiO_x/DLC/DLC:SiO_x/nSi samples. (I type I-V characteristic – sample from S444 set, II type – sample from S424 set and III type –sample from S414 set)

(S414) I-V characteristics revealed, that in the case of the first measurement the main charge transfer mechanisms are Schottky emission and space charge limited current as well as possibly recombination current in low voltages range, Poole-Frenkel emission in middle voltages range and Schottky emission as well as possibly Fowler-Nordheim and/or trap activated tunneling in highest voltages range. It seems, that the influence of the potential barriers in DLC:SiO_x/DLC/DLC:SiO_x superlattice should be taken into account [10, 11]. In the case of the second measurement the main charge transfer mechanisms were Poole-Frenkel emission in lower voltages range and space charge limited current with exponential trap distribution as well as possibly Fowler-Nordheim and/or trap activated tunneling in higher voltages range. It seems, that in the case of the samples with negative resistance range in I-V characteristics, current induced damages resulted in both disappearance of the negative resistance phenomena and contact limited charge transport mechanisms in the samples. While for the samples with no negative resistance phenomena observed, current induced damages resulted in flow of the mixed contact and bulk limited current at lower voltages instead of the contact limited current.

Data on peak current and voltage of the current peak are presented in Fig. 6. The current of the negative resistance peak in all cases was in (0.6 – 0.24) mA range, while voltage of the peak was in 2 V – 4 V range samples of the

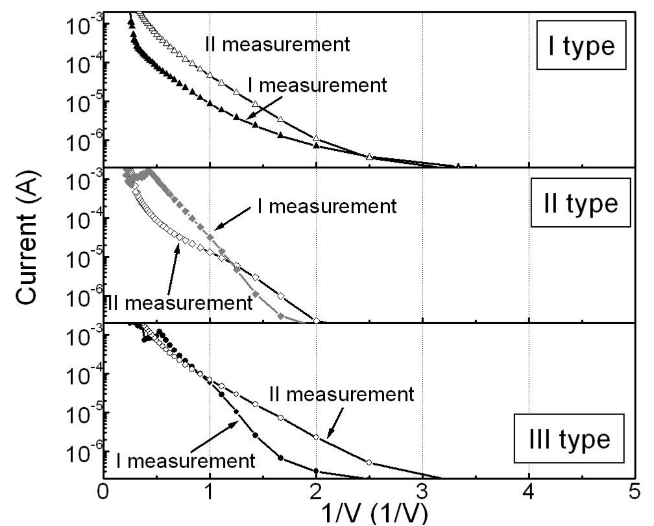

Fig. 4. Trap activated tunneling plot of the forward I-V characteristics of DLC:SiO_x/DLC/DLC:SiO_x/nSi samples. (presented I type I-V characteristic was measured for the sample from S444 set, II type – for the sample from S424 set and III type – for sample from S414 set)

Table 3. ε_{Sch}, ε_{PF} and n values of the forward I-V characteristics of DLC:SiO_x/DLC/DLC:SiO_x/nSi samples

Sample's set	Meas. No	Electric field range (kV/cm)	ε_{Sch}	Electric field range (kV/cm)	ε_{PF}	Electric field range (kV/cm)	n in $J \sim V^n$ plot
S414	1	100 – 350	59.8	100 – 350	<0	100 – 300	0.23
		350 – 550	2.61	350 – 550	23.21	300 – 450	1.58
		550 – 900	0.48	550 – 800	2.07	450 – 800	7.98
		1700 – 2400	3.21	800 – 1700	0.19	800 – 1700	4.8
	2	100 – 300	74.7	100 – 300	<0	100 – 300	0.33
		300 – 650	0.74	300 – 700	4.96	300 – 650	5.56
		650 – 2800	6.88	700 – 1200	30.74	650 – 2800	3.41
S424	1	70 – 350	178.41	70 – 300	<0	70 – 350	0.21
		350 – 800	0.44	300 – 400	51.37	350 – 700	8.1
		800 – 1600	3.21	400 – 600	1.52	700 – 1700	4.44
		1600 – 3000	<0	600 – 1500	14.56	1700 – 2700	<0
		3000 – 3500	3.06	1500 – 3000	<0	2700 – 3500	6.15
				3000 – 3500	16.2		
	2	70 – 300	599.67	70 – 300	<0	70 – 300	0.11
		300 – 550	0.6	300 – 550	3.5	300 – 550	5.95
		550 – 3500	7.14	550 – 2400	70.62	550 – 2300	2.97
				2400 – 3500	178.41	2300 – 2500	9.57
						2500 – 3500	2.88
S444	1	100 – 300	48.95	100 – 350	<0	100 – 300	0.42
		300 – 1000	2.85	350 – 1300	24.81	300 – 1100	3.29
		1000 – 1500	7.14	1300 – 3000	163.24	1100 – 3000	2.72
		1500 – 3000	18.67			3000 – 3600	10.12
	2	100 – 300	84.33	100 – 350	<0	100 – 300	0.3
		300 – 900	1.15	350 – 700	5.27	300 – 800	4.93
		900 – 3000	8.3	700 – 1300	26.57	800 – 3000	3.44
				1300 – 3000	79.26		

sets S414, S424, S444, S222 and in 3.3 V – 7.2 V range for samples of the set S989. It seems, that voltage of the current peak shifted to the higher voltages with increase of the thickness of the DLC:SiO_x/DLC/DLC:SiO_x superlattice layers. Peak current decreased with increase of the peak voltage in the case of the samples of the sets S414, S424, S444, S222. While in the case of the samples of the set S989 there is no pronounced tendency.

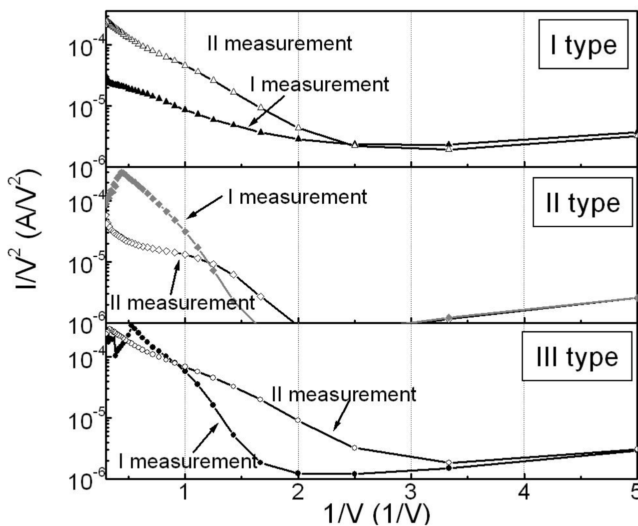

Fig. 5. Fowler-Nordheim tunneling plot of the forward I-V characteristics of DLC:SiO_x/DLC/DLC:SiO_x/nSi samples (presented I type I-V characteristic was measured for the sample from S444 set, II type – for the sample from S424 set and III type – for sample from S414 set)

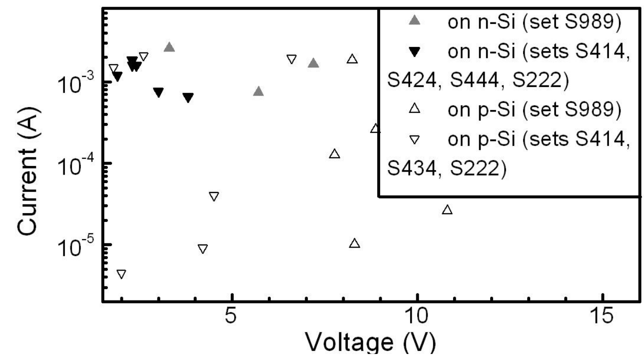

Fig. 6. Negative resistance effect data: peak current strength and voltage of the current peak

3.2. I-V characteristics and charge transfer mechanisms of the diamond like carbon superlattices on p-type silicon

In the case of the DLC:SiO_x/DLC/DLC:SiO_x superlattices fabricated on p-type silicon symmetric or quasi-symmetric I-V characteristics were observed. I-V characteristics of the part of the samples were linear. In other cases non-linear I-V characteristics were observed with turn-on voltage from several volts up to 20 V. For the most samples electric current induced changes of the I-V characteristics – decreased the turn-on voltage or even induced transition to the ohmic conductivity (Fig. 7).

For some DLC:SiO_x/DLC/DLC:SiO_x superlattices fabricated on p-type silicon the negative resistance effect was observed (Fig. 7). That effect was more pronounced

Table 4. ε_{Sch}, ε_{PF} and n values of the forward I-V characteristics of DLC:SiO_x/DLC/DLC:SiO_x/pSi samples

Sample	Meas. No	Electric field range (kV/cm)	ε_{Sch}	Electric field range (kV/cm)	ε_{PF}	Electric field range (kV/cm)	n in $J \sim V^n$ plot
S414	1	650 – 800	0.35	1100 – 1800	118.45	650 – 800	10.6
		800 – 1400	3.84	1800 – 2300	<0	800 – 1800	3.5
		1400 – 1800	7.98	2300 – 2700	48.95	650 – 800	10.6
S434	1	1100 – 1800	11.68	1100 – 1800	118.45	1100 – 1800	2.6
		1800 – 2300	<0	1800 – 2300	<0	1800 – 2300	–7.3
		2300 – 2700	7.14	2300 – 2700	48.95	2300 – 2700	15.9
	2	80 – 300	2	80 – 300	29.61	80 – 900	1.7
		300 – 700	10.2	300 – 1100	1066		
		700 – 1100	66.63				
S989 (III type I-V)	1	2300 – 2400	0.03	2300 – 2400	0.12	2300 – 2400	66.4
		2500 – 3000	66000	2500 – 3000	<0	2500 – 3000	0.06
		3200 – 3500	0.22	3200 – 3500	0.94	3200 – 3500	28.7
		3500 – 4000	1.5	3500 – 4000	7.27	3500 – 4000	11.6
	2	4200 – 6200	2.2	4200 – 6200	10.66	4200 – 6200	11.3
		1700 – 1900	0.27	1700 – 1900	1.18	1700 – 1900	19
		1900 – 2500	3.06	1900 – 2500	17.13	1900 – 2500	6.2
		2500 – 5100	5.44	2500 – 5100	31.94	2500 – 5100	5.9
		5200 – 6200	2.44	5200 – 6200	11.95	5200 – 6200	11.2
S989 (IV type I-V)		2200 – 2400	0.03	2200 – 2400	0.14	2200 – 2400	60.7
		2400 – 3900	3.84	2400 – 3900	21.76	2400 – 3900	6.5
		3900 – 6100	2	3900 – 6100	9.57	3900 – 6100	11.5
		1700 – 1900	0.05	1700 – 1900	0.19	1700 – 1900	46.5
		1900 – 2800	1162	1900 – 2800	<0	1900 – 2800	0.31
		2800 – 3000	1.55	2800 – 3000	7.69	2800 – 3000	10
		3100 – 6500	2.85	3100 – 6500	14.19	3100 – 6500	9.3
		1800 – 1900	0.13	1800 – 1900	0.57	1800 – 1900	27.6
		1900 – 2400	1.47	1900 – 2400	7.54	1900 – 2400	8.87
		2400 – 6500	4.53	2400 – 6500	24.8	2400 – 6500	6.96

than in the case of the samples fabricated on n-Si: peak current was substantially higher than valley current for DLC:SiO_x/DLC/DLC:SiO_x superlattices fabricated on p-type silicon (see Fig. 2). In the case of the DLC:SiO_x/DLC/DLC:SiO_x superlattices fabricated on p-type silicon for some samples negative resistance effect remained after the first measurement. However, in such a case peak current decreased and, sometimes, shift of the current peak voltage was observed.

In the case of the I type sample possible charge transfer mechanisms were analyzed in the voltage range below the current peak voltage (Fig. 7, a, Table 4). There were revealed, that in this case Schottky emission as well as space charge limited current with exponential traps distribution seems to be the main charge transfer mechanisms. However, Fowler-Nordheim and trap activated tunneling mechanisms should be considered as well. No negative resistance effect was observed during the subsequent measurements. I-V characteristics measured during the subsequent measurements were noisy, therefore charge transfer mechanisms analysis was complicated.

In the case of the sample with II type I-V characteristic the main charge transfer mechanism in quasilinear I-V range below the current peak voltage was Fowler-Nordheim tunneling and space charge limited current with the exponential trap distribution ($n = 3.27$) at the lower voltages and space charge limited current ($n = 1.9$) at the higher voltages range (Table 4). Trap assisted current possibly can be considered as well. It seems, that the sample was irreversibly electrically damaged during the first measurement and subsequently substantially increased current and quasilinear I vs V dependence was observed (Fig. 7, b).

Analysis of the III type I-V characteristics revealed linear parts in Schottky emission, Poole-Frenkel, double logarithmic, trap activated tunneling and Fowler-Nordheim plots. However, in the case of the Schottky and Poole Frenkel plots unrealistically high values of the dielectric permittivity were achieved (current increase with voltage was too slow) (Table 4). While in the case of the double logarithmic plot current increase with voltage was relatively sudden ($n > 3.8$ in $J \sim V^n$ plot) (Table 4). It seems, that in this case the main charge transfer mechanisms are Fowler-Nordheim emission and/or trap activated tunneling In the case of the IV type I-V characteristics the main charge transfer mechanisms seems to be Fowler-Nordheim emission and/or trap activated tunneling (Fig. 8).

4. DISCUSSION

In summary I-V characteristics of the multilayer DLC:SiO_x/DLC/DLC:SiO_x/nSi and DLC:SiO_x/DLC/ /DLC:SiO_x/pSi samples were investigated. Diode-like I-V characteristics were observed for the DLC:SiO_x/DLC/ /DLC:SiO_x/nSi structures. The leakage current of the almost all diamond like carbon superlatice and nSi heterostructures was lower than the leakage current of the single layer DLC:SiO_x/nSi heterojunction. Inthe case of the reverse I-V characteristics of single layer DLC:SiO_x/nSi

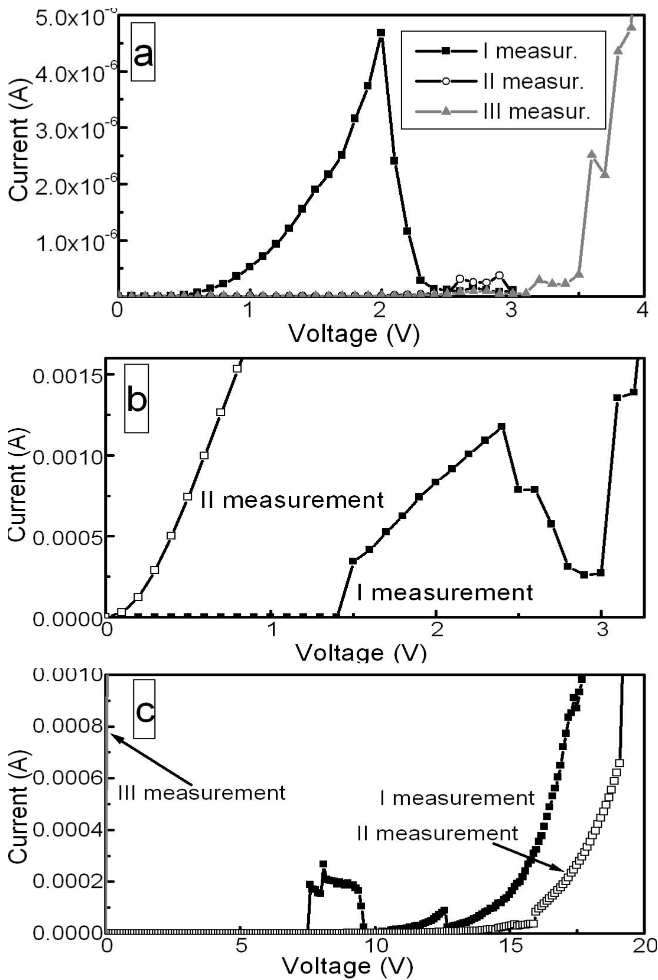

Fig. 7. Typical I-V characteristics of DLC:SiO_x/DLC/DLC:SiO_x superlattices fabricated on p-type silicon: I type (sample's set S414) (a), II type (sample's set S434) (b), III type (sample's set S989)

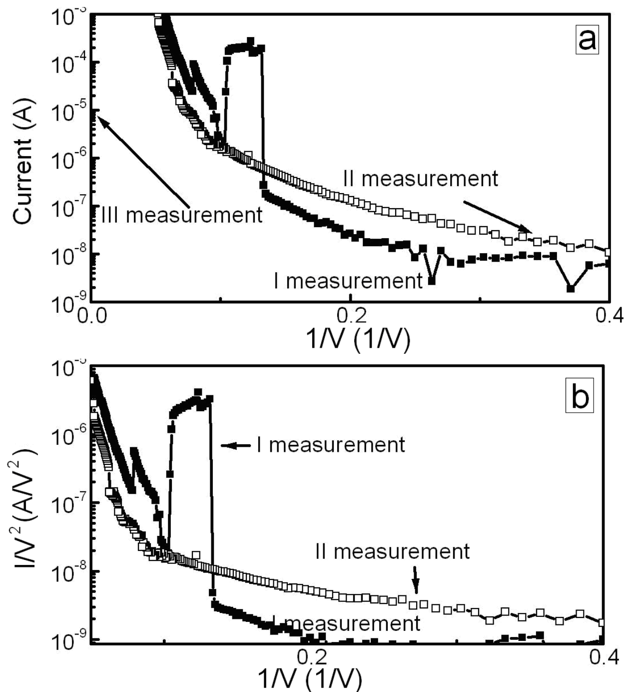

Fig. 8. Trap activated tunneling plot (a) and Fowler-Nordheim plot (b) of the DLC:SiO_x/DLC/DLC:SiO_x superlattice fabricated on p-type silicon: III type I-V characteristics

heterojunction and DLC:SiO_x/DLC/DLC:SiO_x/*n*Si structures some kind of the current steps were detected for most samples investigated. It was explained by different charge transfer mechanisms – Schottky emission in low voltage range and superposition of the space charge limited current and generation current at higher voltages. However, it seems, that electric current flow through the diamond like carbon superlattice results in formation of some additional defects. Such an effect was not observed for a single DLC:SiO_x/*n*Si heterostructure. Therefore, formation of the traps as a result of the damage of the "conventional" DLC interlayer in diamond like carbon superlattice can be assumed. In the case of the forward I-V characteristics for some samples negative resistance effect was observed. However, in most cases these I-V characteristics were unstable. It seems, that the negative resistance phenomenon was more often observed in the case of the samples with thicker intermediate DLC interlayer (≥4 nm). In the case of the samples with negative resistance range in I-V characteristics, current induced damages resulted in both disappearance of the negative resistance phenomena and contact limited charge transport mechanisms in the samples. While for the samples with no negative resistance phenomena observed, current induced damage resulted in flow of the mixed contact and bulk limited current at lower voltages instead of the contact limited current. In the case of the DLC:SiO_x/DLC/DLC:SiO_x superlattices fabricated on p-type silicon symmetric or quasi-symmetric I-V characteristics were observed. For the most samples electric current induced changes of the I-V characteristics – decrease of the turn-on voltage or even transition to the ohmic conductivity. For some DLC:SiO_x/DLC/DLC:SiO_x superlattices fabricated on p-type silicon negative resistance effect was observed). That effect was more pronounced than in the case of the samples fabricated on *n*-Si. In the case of the DLC:SiO_x/DLC/DLC:SiO_x superlattices fabricated on p-type silicon for some samples negative resistance effect remained after the first measurement. Fowler-Nordheim and trap activated tunneling appeared to be the main charge transfer mechanisms in DLC:SiO_x/DLC/DLC:SiO_x/*p*Si samples. Current flow related disappearance of the negative resistance effect possibly can be explained by electrically induced damage of the DLC interlayer. Such a behavior can be explained taking into account case of the negative differential resistance in organic semiconductor based structures and devices [16 – 18]. Negative differential resistance effect was observed in numerous organic semiconductor based structures [16 – 18]. It was explained by strongly inhomogeneous current flow through the filamentary microconducting channels and subsequent decrease of the current due to the strong local heating by current flowing via strongly localized pathways [16 – 18]. Similarly negative differential resistance effect observed for PLD deposited DLC superlattice in [8, 9] was explained by current flow through the sp^2-rich one-dimensional channels within sp^3 bonded carbon matrix. It should be mentioned, that in the case of the organic semiconductors negative resistance phenomena was more stable in comparison with the diamond like carbon superlattices described in present study. Thus negative resistance phenomena observed in

present research for some DLC superlattices possibly can be explained by current flow through the sp^2-rich microconducting channels within mainly sp^3 bonded carbon matrix and local heating that microfilaments by flowing electric current. It seems, that in the case of the diamond like carbon superlattices investigated in present research local heating in local microconducting channels in most cases resulted in irreversible destruction of that localized current pathways. It can be mentioned, that no instability of I-V characteristics was reported for DLC based tunnel diodes in [8, 9]. However, negative resistance peak for PLD deposited DLC superlattice was observed only at 77 K temperature [8]. Negative resistance phenomena were observed at room temperature for nitrogen doped DLC based structure in [9]. However, in that case tunneling via potential barrier at DLC/silicon heterostructure was responsible for the phenomena observed [9].

CONCLUSIONS

In conclusion in present research current-voltage characteristics and charge transfer mechanisms of diamond like carbon based superlattices deposited on n-type and p-type monocrystalline silicon substrates were investigated. Diode-like I-V characteristics were observed for DLC superlattices fabricated on *n*Si, while for DLC superlattices fabricated on p-type silicon symmetric or quasi-symmetric I-V characteristics were observed. In the case of the forward I-V characteristics for some samples fabricated on *n*Si negative resistance effect was observed. For some DLC superlattices fabricated on *p*Si negative resistance effect was observed as well. The negative resistance phenomenon was more often observed in the case of the samples with thicker intermediate DLC interlayer (≥4 nm). However, in most cases that phenomenon was unstable, especially in the case of the samples deposited on *n*Si. Presence of negative resistance phenomena in some DLC superlattices possibly can be explained by current flow through the sp^2-rich microconducting channels within mainly sp^3 bonded carbon matrix and local heating that microfilaments by flowing electric current. Local heating in local microconducting channels in most cases results in irreversible destruction of that localized current pathways.

Acknowledgements

Andrius Vasiliauskas would like to thank for grant in the frames of the project "Promotion of Students' Scientific Activities". Šarūnas Meškinis would like to acknowledge Lithuanian Ministry of Education and Science for the State grant of the researcher.

REFERENCES

1. **Robertson, J.** Diamond-like Amorphous Carbon *Materials Science and Engineering* R 37 2002: pp. 129 – 281.
2. **Barthelmes, R., Beuermann, M., Metzner, D., Schmidt, G., Westerholt, D., Winter, N., Gerstenmaier, Y. C., Reznik, D., Ruff, M., Schulze, H.-J.** Electroactive Passivation of High Power Semiconductor Devices with Punch through Design by Hydrogenated Amorphous Carbon Layers (a-C:H) *Proceedings of 1998 International Symposium on Power Semiconductor Devices & ICs* 1998: pp. 181 – 184.
3. **Luo, J. K., Fu, Y. Q., Le, H. R., Williams, J. A., Spearing, S. M., Milne, W. I.** Diamond and Diamond-like Carbon MEMS *Journal of Micromechanics and Microengineering* 17 2007: pp. S147 – S163.
4. **Tibrewala, A., Peiner, E., Bandorf, R., Biehl, S., Luthje, H.** Longitudinal and Transversal Piezoresistive Effect in Hydrogenated Amorphous Carbon Films *Thin Solid Films* 515 2007: pp. 8028 – 8033.
5. **Meškinis, Š., Gudaitis, R., Kopustinskas, V., Tamulevičius, S.** Electrical and Piezoresistive Properties of Ion Beam Deposited DLC Films *Applied Surface Science* 254 2008: pp. 5252 – 5256.
6. **Meškinis, Š., Gudaitis, R., Tamulevičienė, A., Kopustinskas, V., Šlapikas, K., Tamulevičius, S.** The Investigation of Piezoresistive, Optical and Electrical Properties of Diamond Like Carbon Films Synthesized by Ion Beam Deposition and PECVD *Materials Science* (*Medžiagotyra*) 16 2010: 292 – 297.
7. **Chiang, K. T., Yang, L., Wei, R., Coulter, K.** Development of Diamond-like Carbon-coated Electrodes for Corrosion Sensor Applications at High Temperatures *Thin Solid Films* 517 2008: pp. 1120 – 1124.
8. **Bhattacharyya, S., Henley, S. J., Mendoza, E., Gomez-Rojas, L., Allam, J., Silva, S. R. P.** Resonant Tunnelling and Fast Switching in Amorphous-carbon Quantum-well Structures *Nature Materials* 5 2006: pp. 19 – 22.
9. **Bhattacharyya, S., Silva, S., Ravi, P.** Demonstration of an Amorphous Carbon Tunnel Diode *Applied Physics Letters* 90 2007: 082105.
10. **Meškinis, Š., Šlapikas, K., Gudaitis, R., Tamulevičius, S., Iljinas, A., Gudonytė, A., Gražulevičius, J. V., Getautis, V., Michalevičiūtė, A., Malinauskas, T., Lygaitis, R.** Investigation of the Electrical Characteristics of the Metal / Organic Semiconductor / Metal Structures with Top Contact Configuration *Materials Science* (*Medžiagotyra*) 16 2010: pp. 195 – 201.
11. **Gonon, P., Deneuville, A., Fontaine, F., Gheeraert, E.** Electrical Conduction and Deep Levels in Polycrystalline Diamond Films *Journal of Applied Physics* 78 1995: pp. 6633 – 6638.
12. **Houng, M. P., Wang, Y. H., Chang, W. J.** Current Transport Mechanism in Trapped Oxides: a Generalized Trap-assisted Tunneling Model *Journal of Applied Physics* 86 1999: pp. 1488 – 1491.
13. **Anatoly, A., Grinberg, Luryi, S., Pito, M. R., Schryer, N. L.** Space-charge-Limited Current in a Film *IEEE Transactions on Electron Devices* 36 1989: pp. 1162 – 1170.
14. **Taylor, D. M.** Space Charges and Traps in Polymer Electronics *IEEE Transactions on Dielectrics and Electrical Insulation* 13 2006: pp. 1063 – 1073.
15. **Miranda, E., Suñé, J., Rodríguez, R., Nafría, M., Aymerich, X.** Breakdown and Anti-breakdown Events in High-field Stressed Ultrathin Gate Oxides *Solid-State Electronics* 45 2001: pp. 1327 – 1332.
16. **Lebedev, E., Forero, S., Brütting, W., Schwoerer, M.** Switching Effect in Poly(*p*-phenylenevinylene) *Synthetic Metals* 111 – 112 2000: pp. 345 – 347.
17. **You, Y. T., Wang, M. L., Xuxie, H. N., Wu, B., Sun, Z. Y., Hou, X. Y.** Conductance-dependent Negative Differential Resistance in Organic Memory Devices *Applied Physics Letters* 97 2010: 233301.
18. **Berleb, S., Batting, W., Schwoerer, M.** Anomalous Current-voltage Characteristics in Organic Light-emitting Devices *Synthetic Metals* 102 1999: 1034 – 1037.